Crystal Structure of Spinach Chloroplast Fructose-1,6-bisphosphatase at 2.8 Å Resolution[†,‡]

Vincent Villeret,[§] Shenghua Huang,[§] Yiping Zhang,[∥] Yafeng Xue,[⊥] and William N. Lipscomb*[,§]

Gibbs Chemical Laboratory, Harvard University, 12 Oxford Street, Cambridge, Massachusetts 02138, Syntex Discovery Research, 3401 Hillview Avenue, Palo Alto, California 94303, and Department of Molecular Biology, Uppsala BMC, S-751 24 Uppsala, Sweden

Received December 15, 1994; Revised Manuscript Received January 27, 1995[⊗]

ABSTRACT: The three-dimensional structure of the spinach chloroplast fructose-1,6-bisphosphatase (Fru-1,6-Pase) has been solved by the molecular replacement method at 2.8 Å resolution and refined to a crystallographic *R* factor of 0.203. The enzyme is composed of four monomers and displays pseudo *D*2 symmetry. Comparison with the allosteric Fru-1,6-Pase from pig kidney shows orientationally displaced dimers within the quaternary structure of the chloroplast enzyme. When the C1C2 dimers of the two enzymes are superimposed, the C3C4 dimer of the chloroplast enzyme is rotated 20° and 5° relative to the C3C4 dimer of the R and T forms of the pig kidney enzyme, respectively. This new quaternary structure, designated as S, may be described as a super-T form and is outside of the pathway of the allosteric transition which occurs in the pig kidney enzyme, which shows a 15° rotation between T and R forms. Chloroplast Fru-1,6-Pase, unlike the pig kidney enzyme, is insensitive to allosteric transformation by AMP. Structural changes in the AMP binding site involving mainly helices H1, H2, and H3 and the loop between H1 and H2 at the dimer interface interfere with binding of the phosphate of AMP. Finally, the location of cysteines residues provides a basis for a preliminary discussion of the activation of the enzyme by reduction of cysteines via the ferredoxin−thioredoxin *f* system; this process is complementary to activation by pH changes, Mg^{2+} or Ca^{2+}, Fru-1,6-P_2, and possibly Fru-2,6-P_2.

Fructose-1,6-bisphosphatase catalyzes the hydrolysis of D-fructose 1,6-bisphosphate (Fru-1,6-P_2) to D-fructose 6-phosphate (Fru-6-P)[1] and inorganic phosphate. One striking feature of Fru-1,6-Pases is the way in which they are regulated. Mammalian Fru-1,6-Pases are key enzymes in the gluconeogenesis pathway and are tightly regulated by two synergistic inhibitors: AMP at an allosteric site and fructose 2,6-bisphosphate (Fru-2,6-P_2) at the active site (Marcus, 1981; Pilkis et al., 1981; Van Schaftingen & Hers, 1981; Benkovic & deMaine, 1982; Tejwani, 1983; Van Schaftingen, 1987). The enzymes require divalent metal ions such as Mg^{2+}, Mn^{2+}, Co^{2+}, or Zn^{2+} for catalytic activity (Gomori, 1943; Kirtley & Dix, 1971; Benkovic & de Maine, 1982). Crystallographic studies of pig kidney Fru-1,6-Pase indicate *D*2 symmetry for the tetramer. Each monomer has 335 amino acid residues. Structures of complexes of Fru-1,6-Pase establish two quaternary conformations, the R and T forms, which differ by a 15°−17° rotation of the lower dimer C3C4 relative to the upper dimer C1C2 (Ke et al., 1990a,b, 1991a). The R form structures include Fru-1,6-Pase complexed with Fru-6-P (2.1 Å resolution) (Ke et al., 1991b), Fru-2,6-P_2 (2.6 Å resolution) (Liang et al., 1992), Fru-1,6-P_2 (2.5 Å resolution), 2,5-anhydroglucitol 1,6-bisphosphate (AhG-1,6-P_2, 2.6 Å resolution), and 2,5-anhydromannitol 1,6-bisphosphate (AhM-1,6-P_2, 2.6 Å resolution) (Zhang et al., 1993). The T form structures include the AMP complex (2.5 Å resolution) (Ke et al., 1991a), the Fru-6-P−AMP−Mg^{2+} complex (2.5 Å resolution) (Ke et al., 1990a), and the Fru-2,6-P_2−AMP−Zn^{2+} complex (2.1 Å resolution) (Xue et al., 1994). Kinetic and structural results show that binding of AMP alone at an allosteric site is sufficient to lock the enzyme into the T form, whereas binding of inhibitors such as Fru-6-P and Fru-2,6-P_2 to the active site does not change the quaternary structure as normally seen as the R form.

In higher plants two Fru-1,6-Pases are necessary for photosynthesis to take place. The first enzyme, located in the cytosol, is involved in sucrose synthesis from triose phosphates exported from the chloroplasts. This enzyme resembles its mammalian counterpart, in being inhibited by Fru-2,6-P_2 and AMP (Zimmerman et al., 1976; Harbron et al., 1981; Herzog et al., 1984). The second enzyme, which is insensitive to AMP, is found within chloroplasts and takes part in the regeneration of ribulose in the reductive pentose phosphate cycle (Benson−Calvin cycle) (Preiss et al., 1967; Halliwell, 1981). The chloroplast Fru-1,6-Pase is activated by light-mediated processes such as reduction of disulfide groups via the ferredoxin−thioredoxin *f* system, pH changes, divalent cation levels, and also perhaps by Fru-2,6-P_2 (Zimmerman et al., 1976; Buchanan, 1980; Meunier et al., 1981; Pradel et al., 1981; Hertig & Wolosiuk, 1983; Soulié et al., 1988, 1991; Ballicora & Wolosiuk, 1990; Ladror et al., 1990; Chardot & Meunier, 1991).

[†] This work is supported by Grant GM 06920 (W.N.L.) from the National Institutes of Health.

[‡] The coordinates have been deposited in the Brookhaven Protein Data Bank (PDB entry code: 1SPI).

* To whom correspondence should be addressed.

[§] Harvard University.

[∥] Syntex Discovery Research.

[⊥] Uppsala BMC.

[⊗] Abstract published in *Advance ACS Abstracts,* March 15, 1995.

[1] Abbreviations: Fru-1,6-Pase, fructose-1,6-bisphosphatase; Fru-1,6-P_2, fructose 1,6-bisphosphate; Fru-2,6-P_2, fructose 2,6-bisphosphate; Fru-6-P, fructose 6-phosphate; AMP, adenosine monophosphate.

0006-2960/95/0434-4299$09.00/0

Dithiothreitol (DTT) slowly activates the enzyme, mimicking the activation of Fru-1,6-Pase by reduced thioredoxin (Hertig & Wolosiuk, 1980; Clancey & Gilbert, 1987). Nevertheless, both the reduced and oxidized form of the enzyme can also be stimulated by agents such as fructose 1,6-bisphosphate, Mg^{2+}, Ca^{2+}, and Ca^{2+}/Fru-1,6-P_2 (Chardot & Meunier, 1991). Moreover, reduction of disulfide groups is not necessarily required to obtain a full activation of the enzyme: Ricard and co-workers (Soulié et al., 1988, 1991) have shown that it is possible to obtain activation of chloroplast Fru-1,6-Pase using potentially physiological amounts of fructose-2,6-P_2 at the pH of chloroplast stroma under light conditions. Such a mechanism might be complementary to the regulation of Fru-1,6-Pase by the oxydoreduction process, since the rate of activation of the enzyme by dithiothreitol is strongly increased by Fru-2,6-P_2 and magnesium. However, there is not yet direct evidence which proves that Fru-2,6-P_2 is involved in the regulation of carbon metabolism in the chloroplast. All of these activation processes are pH dependent: oxidized Fru-1,6-Pase is fully active at pH 8.8, without any reducing agent (Zimmerman et al., 1976). Even though our current knowledge of the regulation of spinach chloroplast Fru-1,6-Pase is still incomplete, there is little doubt that the enzyme is a target of the thioredoxin reductase/thioredoxin system. However, it is unclear if other regulation processes are involved under light/dark transitions.

Sequence comparison of chloroplast and mammalian Fru-1,6-Pases shows a sequence insert of 12−17 amino acid residues near the middle of the primary structure of the chloroplast enzymes (Marcus et al., 1988). Two cysteines are close to this sequence insert and are separated by only four amino acids residues (Cys-Val-Val-Asn-Val-Cys), a characteristic feature of some other enzymes containing redox-active cysteines, e.g., mercuric reductase, glutathione reductase, lipoamide dehydrogenase, and $NADP^+$-malate dehydrogenase. This unusual characteristic and the conservation of these cysteines in all known chloroplast Fru-1,6-Pases led to the proposal that these residues may be implicated in the light-dependent reductive activation process (Marcus et al., 1988).

The present study was carried out in order to provide structural information about the spinach chloroplast Fru-1,6-Pase. We report here the crystallographic structure refined at 2.8 Å resolution of the chloroplast Fru-1,6-Pase and its structural comparison with the pig kidney enzyme in both the T and R states. We also discuss the insensitivity of this enzyme to AMP and its regulation by reduction of cysteines which have now been located in the three-dimensional structure.

MATERIALS AND METHODS

Purification, Crystallization, and Data Collection. Spinach leaves were purchased from a local market. Chloroplast Fru-1,6-Pase was purified following the method of Marcus et al. (1987), slightly modified in steps 4 and 6. A DEAE-cellulose hanger from Pierce, equilibrated with 50 mM Tris-HCl buffer (pH 7.5) containing 0.25 mM EDTA and 0.1 M NaCl, was used in step 4 instead of a Whatman DE-52 DEAE-cellulose equilibrated with Hepes buffer. In order to increase the purity of the preparation, an additional step (step 6) was applied involving a fast liquid chromatography on a Pharmacia mono Q column (2.5 × 11.5 cm) equilibrated with 50 mM Tris-HCl buffer (pH 7.5) containing 0.25 mM EDTA and 0.1 M NaCl. Elution was performed using a linear gradient of NaCl (0.1−0.7 M). The enzyme eluted as two peaks at about 0.48 M NaCl and 0.53 M NaCl. The first peak corresponded to 40% of the total amount of chloroplast Fru-1,6-Pase and was devoid of enzymatic activity. Crystallization trials failed with this fraction. The second peak showed activity at pH 8.5 in the presence of Mg^{2+} and was pure on the basis of SDS−PAGE analysis. Crystals were obtained using this second fraction.

Crystals of chloroplast Fru-1,6-Pase were grown at room temperature by dialyzing the enzyme solution (10−15 mg/mL) against a buffer containing 80 mM NaAc, 0.3 mM $(NH_4)SO_4$, 0.3 mM (Na) citrate, 2% (w/v) PEG (1450), 2% (w/v) PEG (3350), 4 mM NaN_3, 0.2 mM EDTA, and 0.3 mM octylphenoxypoly(ethoxyethanol) (Triton X-100) at pH 5.2. We have also grown crystals in the presence of 1mM AMP in order to test whether AMP binds to the enzyme. Some 7−10 days of dialysis produced crystals which have typical dimensions of 0.2 × 0.4 × 0.6 to 1.0 mm. The space group is $P2_1$, and the unit cell dimensions are a = 76.1 Å, b = 85.7 Å, c = 105.8 Å, $\alpha = \gamma = 90°$, and β = 103.1°. One oligomer consisting of four monomers (358 amino acids residues for each monomer) is present in the crystallographic asymmetric unit.

The diffraction data were collected with a Rigaku R-axis image plate area detector using Cu Kα radiation produced by a rotating anode generator Rigaku Ru200 running at 5.4 kW and located at Professor Ke's laboratory (School of Medicine, University of North Carolina, Chapel Hill). Data were collected for crystals grown with and without AMP. Data from three crystals obtained in the presence of AMP were collected resulting in 29 281 unique reflections between 15 and 2.7 Å resolution (with an R_{merge} of 0.106). These data (referred to as data1) are 83.3% complete between 15 and 2.8 Å resolution. Data from two crystals grown without AMP were also collected, resulting in 23 262 unique reflections between 15 and 2.7 Å resolution (R_{merge} of 0.104). The completeness of this second data set is only 66% between 15 and 2.8 Å resolution. Data were processed with the Rigaku R-axis software package.

Structure Determination. The structure was solved by the molecular replacement method, based on the 43% sequence identity between pig kidney and spinach chloroplast Fru-1,6-Pases. Two search models were used in the molecular replacement procedure: a polyalanine T form pig kidney Fru-1,6-Pase tetramer and a polyalanine R form pig kidney Fru-1,6-Pase tetramer. Two molecular replacement software packages were also used to investigate the rotational and translational parameters: the X-PLOR 3.1 program with the PC refinement protocol (Brunger, 1990) and the automated molecular replacement method of the AMoRe package (Navaza, 1993). The results obtained for the rotational search with the T form polyalanine model using AMoRe were unambigous, the first solution being 2σ above the second one. On the other hand, similar investigation using X-PLOR gave no clear unique solution, even after PC refinement. Comparison of AMoRe and X-PLOR rotation results showed that one of the four best orientations obtained after PC refinement was equivalent to the AMoRe solution. The rotational search where the enzyme was modeled as a polyalanine R form failed using the two molecular replace-

ment packages. As mentioned above, the T and R forms of pig kidney Fru-1,6-Pase differ by a rotation of 15°−17° of one dimer relative to the other. It became clear at this stage that the spinach chloroplast enzyme displays a quaternary structure which is more like the T form pig kidney enzyme than the R form. In order to confirm these results, a third rotational search using AMoRe was done with a polyalanine R form pig kidney Fru-1,6-Pase dimer. As expected, the two rotational solutions converged to a tetramer form reasonably close to the T form pig kidney Fru-1,6-Pase.

Crystals grown with or without AMP gave essentially the same X-ray diffraction intensities. These results show that AMP does not promote the conformational change which had been found previously for pig kidney Fru-1,6-Pase upon binding of this ligand.

A translational search followed by a rigid body minimization of the four monomers in the asymmetric unit gave an *R* factor of 0.48 between 15 and 2.8 Å. Results from X-PLOR or AMoRe were similar. At that point the refinement was pursued with our most complete data set (data1). Forty cycles of positional refinement of the polyalanine model between 15 and 2.8 Å lowered the *R* factor to 0.35. Noncrystallographic symmetry averaging was then applied in order to improve the first electron density map. The averaged map permitted an unambigous assignment of sequence. The model was built using the molecular graphic package O (Jones et al., 1991). A first cycle of simulated annealing using data between 10 and 2.8 Å (with I/σ greater than 2) brought the *R* factor to 0.235. The inclusion of the low resolution terms (10−6 Å) in the refinement helped to identify electron density corresponding to the 170's loop (residues 150−180) in monomer C2. No clear density was observed for this loop in monomers C1, C3, and C4. A second averaged electron density map was calculated, and some manual corrections were applied to the model. However, no electron density for the 170's loops was observed in the averaged map, even in monomer C2. This lack of density suggested that the 170's loops have different conformations and do not follow the 222 noncrystallographic symmetry. A second cycle of simulated annealing using the model built in the averaged map but in which the 170's loop of monomer C2 was included brought the *R* factor to 0.225. Electron density for 170's loops in monomers C1, C3 and C4 was identified. A third cycle of simulated annealing using data between 6.0 and 2.8 Å resolution gave a final *R* factor of 0.203. At the resolution of 2.8 Å, no water molecules were added to the model.

The overall *B* factor for the whole structure is 28 Å^2, and root-mean-square deviations from ideal geometries for bond lengths and bond angles are 0.019 Å and 2.25°, respectively. In order to perform a quantitative evaluation of the fit of the atomic model into the electron density map, the real-space *R* factor was computed using the algorithm described by Jones and co-workers (1991). For most residues in the structure the fit is very good. However, strand B2 (residues 113−118), which is solvent exposed, is poorly defined. Also the electron density is moderately good in loops around residues 240, 295, and 330. The loop between residues 150 and 180 (referred to as 170's loop) is well defined in monomers C2 and C3 but shows breaks around residues 162, 167, and 170 in monomer C4. This loop is poorly defined between residues 159 and 168 in monomer C1. The four 170's loops display different conformations and are involved in crystal packing contacts. Also, the five N-terminal residues are disordered. In addition, weak electron density is observed for residues 6−11 in monomer C1, and these same residues are disordered in the three other monomers. No reasonable density was found for the loop between residues 61 and 82. This loop has been identified as a proteolytically sensitive region for all Fru-1,6-Pases; no significant density was found for the structurally similar loop in the crystal structure of pig kidney or human liver Fru-1,6-Pases.

RESULTS

The spinach chloroplast Fru-1,6-Pase is a tetramer with pseudo *D*2 symmetry. Each of the four polypeptide chains has 358 amino acids residues (39 164 Da) and consists of 9 α-helices and 13 β-strands. These elements of secondary structure, similar to those in the pig kidney enzyme, are arranged in layers, from bottom up (Figure 1): 3 α helices (H1, H2, H3), eight-stranded β-sheet (β-sheet 1 in Figure 1: B8, B7, B6, B5, B4, B3, B1, B2, from the left to the right, respectively), 2 α-helices (H7, H8), five-stranded β-sheet (B9−B13) and 2 α-helices (H6, H9). The residue ranges for these secondary structures are given in Table 1. On the basis of structural studies of the pig kidney enzyme, each monomer has two domains, the AMP domain of residues 1−200 and the FBP domain of residues 201−335 (1−226 and 227−358 in the chloroplast enzyme). The active sites are located in the FBP domain near the interface between two monomers. Metal ions bind near the interface between the FBP and AMP domains. The binding site of AMP identified in the pig kidney Fru-1,6-Pase is located between the helices H1, H2, H3 and the eight-stranded β-sheet and is shown in Figure 1 as the symbol "*". Seven cysteine residues are found within the monomer: Cys^{51} (helix H2), Cys^{94} (helix H3), Cys^{155}, Cys^{174}, Cys^{179} (170's loop), Cys^{191} (strand B5), and Cys^{307} (helix H8). These residues are also shown in Figure 1.

In order to compare their quaternary conformations, three-dimensional structures of T (pig kidney Fru-1,6-Pase complexed with AMP-Fru-2,6-P_2 and Zn^{2+}) (Xue et al., 1994), R (pig kidney Fru-1,6-Pase complexed with Fru-6-P) (Ke et al., 1991b), and S (the spinach chloroplast Fru-1,6-Pase) forms are oriented so that their geometric centers superimpose on the coordinate origin, and their three molecular 2-fold axes correspond to the *x*, *y*, and *z* axes. The four monomers are labeled clockwise as C1, C2, C3 and C4 (Figure 2).

The R and T forms of the pig kidney enzyme display *D*2 symmetry, and for these two structures the molecular *y* axis is also a crystallographic 2-fold symmetry axis: the R form crystallizes in the space group $P3_221$ with one C1C2 dimer in the asymmetric unit; the T form crystallizes in the space group $P2_12_12$, also with one C1C2 dimer in the asymmetric unit. On the other hand, one tetramer of the S form of the chloroplast enzyme is present in the asymmetric unit of the $P2_1$ crystals. The overall root mean square (rms) difference between the four chains (without the insertion between residues 158 and 174) is 1.2 Å. The secondary structure elements of the C2, C3, and C4 monomers of the S form are superimposed on the C1 monomer after rotations of 179.8°, 176.7°, and 178.8° around *x*, *y*, and *z*, respectively. At the current resolution (2.8 Å) the differences from the exact *D*2 symmetry also reflect coordinates errors. Although

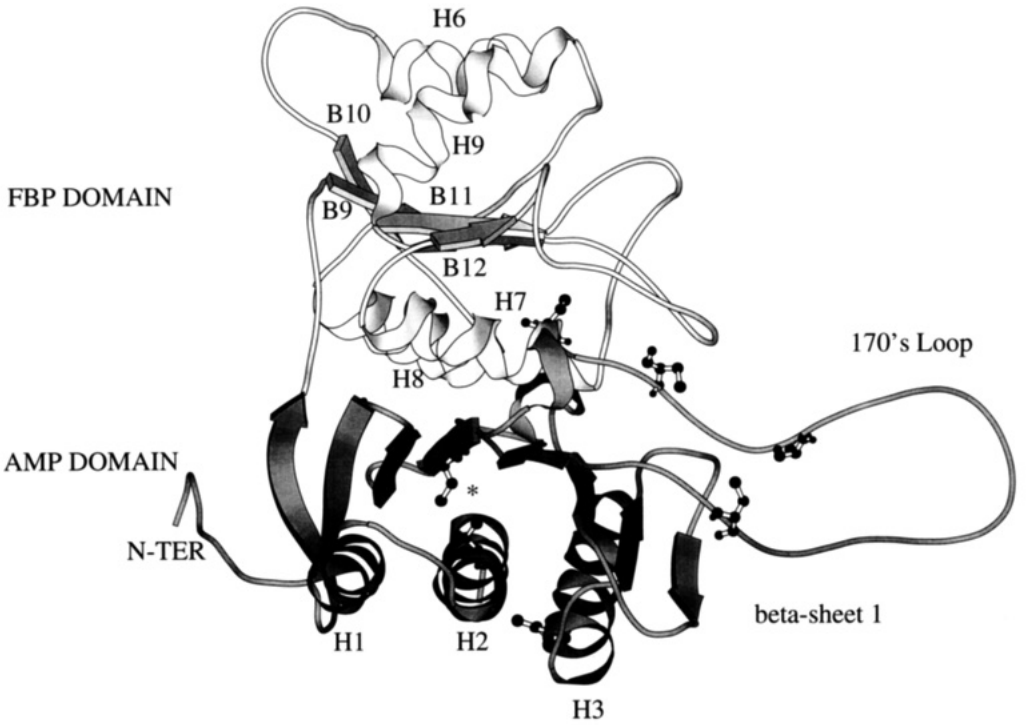

FIGURE 1: Ribbon drawing showing the secondary structures and loops of the chloroplast Fru-1,6-Pase. Five layers of secondary structures are identified, from the bottom up: helices H1, H2, and H3; eight-stranded β-sheet (β-sheet 1); helices H7 and H8; five-stranded β-sheet (B9−B13) and helices H6 and H9. Cysteines at positions 51 (helix H2), 94 (helix H3), 155, 174, 179 (170's loop), 191 (strand B5), and 307 (helix H8) are shown. The picture has been generated using Molscript.

Table 1: Residue Range of Secondary Structures in the Pig Kidney and Spinach Chloroplast Fru-1,6-Pases

secondary structure	pig kidney Fru-1,6-Pase	chloroplast Fru-1,6-Pase	secondary structure	pig kidney Fru-1,6-Pase	chloroplast Fru-1,6-Pase
H1	12−24	22−34	B7	181−187	207−213
H2	28−50	38−60	B8	192−199	218−225
H3	72−88	82−98	B9	207−210	233−236
B1	92−95	102−105	H6	221−232	247−258
B2	103−106	113−116	B10	240−243	266−269
B3	113−118	123−128	H7	247−258	273−284
H4	123−127	133−137	B11	260−264	286−290
B4	132−139	142−149	H8	276−291	305−317
H5	149−153	181−185	B12	294−296	320−322
B5	160−167	186−193	B13	316−319	342−345
B6	171−176	197−202	H9	320−332	346−358

we cannot accurately estimate the degree of intrinsic or induced structural asymmetry, the 3.3° deviation observed around the *y* axis is significant and may reflect some deviation from the *D*2 symmetry for the S form enzyme.

The overall root mean square (rms) difference for backbone atoms of the secondary structures between the chloroplast enzyme and the R and T forms (after superimposing the FBP domains) is 1.8 and 1.7 Å, respectively. The rms difference between each element of secondary structure is given in Table 2. Larger deviations are observed for helices H1, H3, H4, H5, and H6 and for strands B1, B2, and B3. Differences in loops also occur between the two enzymes: the loops between helices H1 and H2 and between strand B9 and helix H6 display different conformations. The major difference is the 170's loop which shows an insertion of 16 residues between residues 158 and 174 (148 and 149 in pig kidney sequence). Also the 170's loops have different conformations in the four monomers of the chloroplast enzyme (Figure 3).

The R-to-T transition of mammalian Fru-1,6-Pases is triggered by binding of AMP to the allosteric sites: extensive structural changes occur during the allosteric transition and have been described elsewhere (Liang et al., 1993; Zhang et al., 1994). The most spectacular reorganization is a 15° rotation around the *z* axis of the C3C4 dimer relative to the upper C1C2 dimer. As mentioned previously, the S form displays a quaternary conformation which is considerably closer to the T form than to the R form. The chloroplast enzyme has a new quaternary structure in the sense that the C3C4 dimer of the S form rotates 20° relative to the C3C4 dimer of the R form and 5° relative to the C3C4 dimer of the T form when C1C2 dimers are superimposed (Figure 4): the quaternary structure of the S form may therefore be described as a "super T" form. These differences in the relative orientation of C3C4 and C1C2 dimers are explained in part by extensive changes within the monomer: during the R to T allosteric transition of pig kidney Fru-1,6-Pase, major structural changes are observed for helices H1, H2, and H3 which belong to the AMP domain. These helices are at the interfaces between the C1C2 and the C3C4 dimers and are directly implicated in the relative rotation of the dimers during the allosteric transition (Liang et al., 1993;

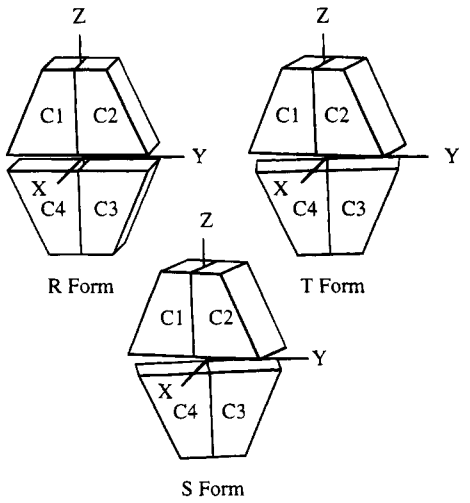

FIGURE 2: Schematic representation of the R, T, and S forms of the Fru-1,6-Pase tetramer. The monomers are labeled clockwise as C1, C2, C3, and C4. The *x*, *y*, and *z* axes correspond to the molecular axes. These tracings illustrate the 15° and 20° rotation of the C3C4 dimer relative to the C1C2 dimer observed between the T and R forms and the S and R forms, respectively.

Table 2: Root Mean Square (rms) Differences between Backbone Atoms for Each Secondary Structure of the T or R States of Pig Kidney and the Spinach Chloroplast (S) Fru-1,6-Pases

secondary structure	rms (Å) T − S	rms (Å) R − S	secondary structure	rms (Å) T − S	rms (Å) R − S
H1	2.3	3.0	B7	1.0	1.5
H2	1.4	1.2	B8	1.5	1.5
H3	2.4	2.6	B9	1.0	0.9
B1	2.9	3.2	H6	2.1	2.1
B2	3.6	4.3	B10	0.9	0.7
B3	1.9	1.9	H7	0.8	0.8
H4	2.3	3.1	B11	0.7	0.7
B4	0.8	0.9	H8	0.7	0.6
H5	1.7	1.8	B12	0.6	0.5
B5	0.9	1.0	B13	0.7	0.6
B6	1.0	1.1	H9	1.5	1.6

Zhang et al., 1994). These helices display quite different positions in the S form: if we superimpose the FBP domains of the T and S forms, helices H1, H2, and H3 rotate 7°, 7.5°, and 13° around axes (0.05, 0.98, 0.19), (0.36, 0.87, 0.52), and (0.04, 0.46, 0.88) and translate along axes (1.03, 1.18, −1.42), (−1.67, 1.68, −0.31), and (−3.02, 2.45, −0.83), respectively. H1 and H2 move nearly as a rigid body in the same direction, away from helix H3.

AMP Binding Site. No density corresponding to AMP molecules was found in the electron density map. AMP does not bind to the enzyme, as suggested by its insensitivity to this ligand (Preiss et al., 1967; Halliwell, 1981). Within individual monomers of the T form, AMP binds between helices H1, H2, and H3 and the eight-stranded β-sheet of the AMP domain. The different positions of helices H1, H2, and H3 in the S form explain its insensitivity to AMP: the reorientations of H1 and H2 move the H1−H2 loop toward the phosphate binding position observed in the T form. The B3 strand which is involved in the binding of AMP and in the transmission of the allosteric signal to the active site in the pig kidney enzyme has a slightly different conformation in the S form, as it moves away from the AMP binding site. Moreover, residues which interact with AMP in the pig kidney enzyme are not conserved in the chloroplast Fru-1,6-Pase. In the T form, the phosphate group of AMP

FIGURE 3: Cα tracing of (from top to bottom) C1, C3, and C4 monomers (thin lines) superimposed onto C2 (thick lines). The loops between residues 150 and 180 are located on the left. The different conformations for these loops are clearly visible.

interacts with Thr^{27}, Glu^{29}, Met^{30}, Lys^{112}, and Tyr^{113} (Liang et al., 1993; Zhang et al., 1994); residues at equivalent positions in the S form are Asp^{37}, Glu^{39}, Leu^{40}, Asn^{122}, and Tyr^{123}, respectively; only two of these residues ($Glu^{29(T)\text{-}39(S)}$ and $Tyr^{113(T)\text{-}123(S)}$) are conserved between the two enzymes. The adenine group of AMP is in a hydrophobic environment surrounded by residues from helices H1 and H2 and the β-turn 177−180. Movements of H1 and H2 nearly as a rigid body result in a tightened cavity between helices H1-H2-H3 and the eight-stranded β-sheet.

Active Site. The active site has been defined from various complexes of pig kidney Fru-1,6-Pase with substrate or substrate analogues and metal ions (Zhang et al., 1993). It is located in the FBP domain near the interface between two monomers related by a 180° rotation around the *z* axis (C1C2 and C3C4). The active site of each monomer can be divided in three parts, the 6-phosphate binding region, the sugar ring binding region, and the 1-phosphate and metal binding region. Metal ions bind near the interface between the FBP and AMP domains within one monomer. The residues which define the active site in the pig kidney Fru-1,6-Pase are Asp^{121} and Gly^{122} (strand B3), Asn^{212} and Tyr^{215} (loop B9−

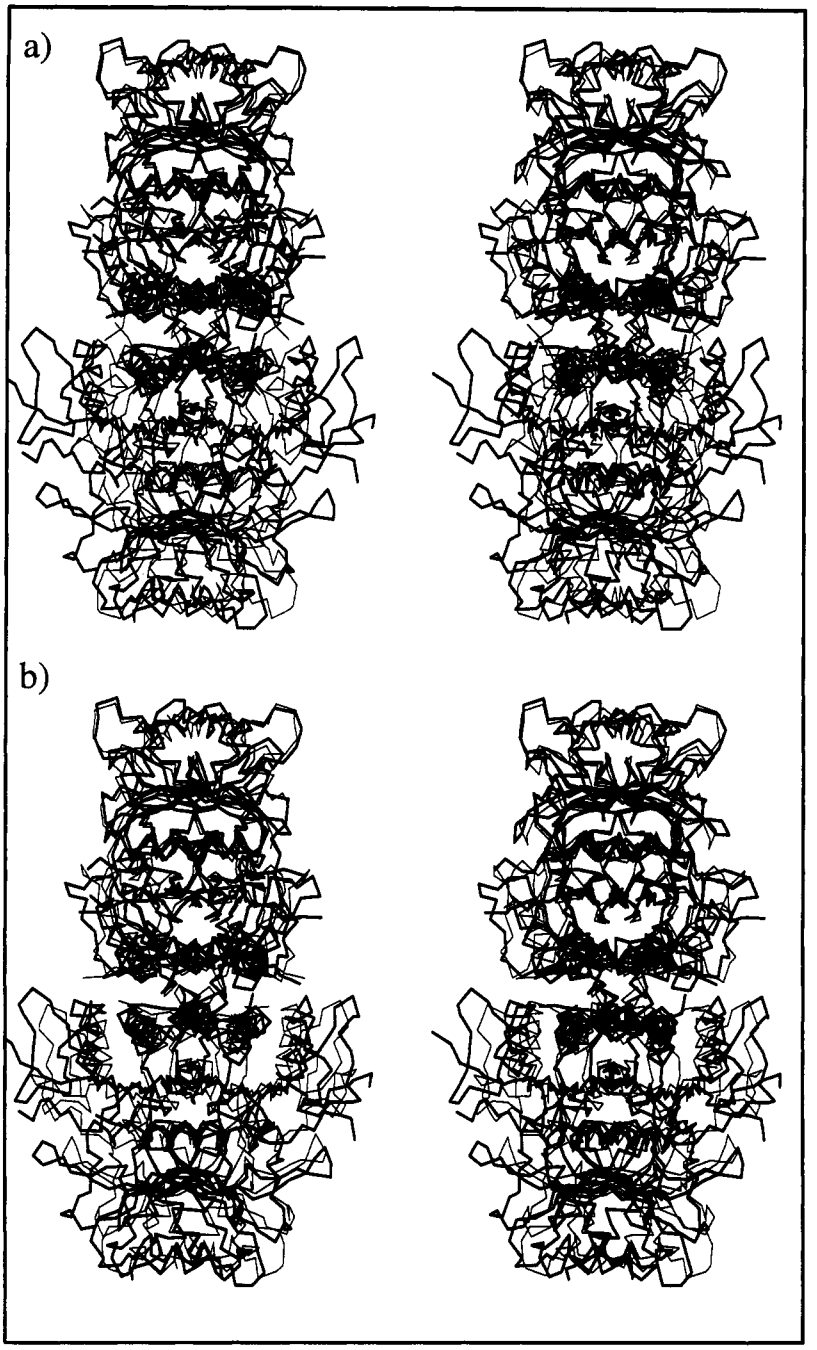

FIGURE 4: Stereoviews of (a) Cα atoms of the R state of pig kidney Fru-1,6-Pase (thin lines) and the spinach chloroplast Fru-1,6-Pase (thick lines). (b) Cα atoms of the T state of pig kidney Fru-1,6-Pase (thin lines) and the spinach chloroplast Fru-1,6-Pase (thick lines). The tetramers are viewed along the *y* axis. The C1C2 dimers of the two enzymes have been superimposed at the top of each stereoview. For clarity, the 170's loops in the chloroplast enzyme are not shown. These Cα tracings show the 20° and 5° rotation of C3C4 dimer relative to C1C2 dimer between the chloroplast Fru-1,6-Pase and the pig kidney R and T states.

H6), Arg^{243} and Tyr^{244} (loop B10−H7), Tyr^{264} (strand B11), Lys^{274} (helix H8), Arg^{276} (helix H8), and the backbone NH of Met^{248} (helix H7). Most of these residues are strictly conserved in the chloroplast enzyme, except for Tyr^{215} and Met^{248} which are replaced by Asn (position 241) and Leu (position 274), respectively. Overall root mean square differences for these residues between the two enzymes are low (0.3−0.7 Å), except for Asp^{121} (position 131 in chloroplast Fru-1,6-Pase) and Gly^{122} (position 132) which show rms differences of 1.28 and 2.6 Å, respectively. These residues are close to the 1-phosphate and metal binding region. In pig kidney Fru-1,6-Pase, Asp^{121} and Gly^{122} are at the beginning of helix H4 which is an important element in the signaling pathway between AMP and active site domains: during the R to T transition, residues 123−127 (helix H4) move between 1.0 and 2.5 Å, giving a somewhat tightened active site cavity in the T form and creating new interactions involving Asp^{121} and also between C1 and C2 active sites (Xue et al., 1994). Site-directed mutagenesis of Gly^{122} also suggests that this residue is at a hinge point adjacent to helix H4 and is important for signal transmission between the AMP site and the active site (Zhang et al., 1995). When Gly^{122} is mutated to Ala, the affinity of the enzyme for AMP (which binds 28 Å away from this region) is strongly reduced (the K_i for this ligand is increased 80-fold), and the cooperativity for Mg^{2+} is abolished. Helix H4 in

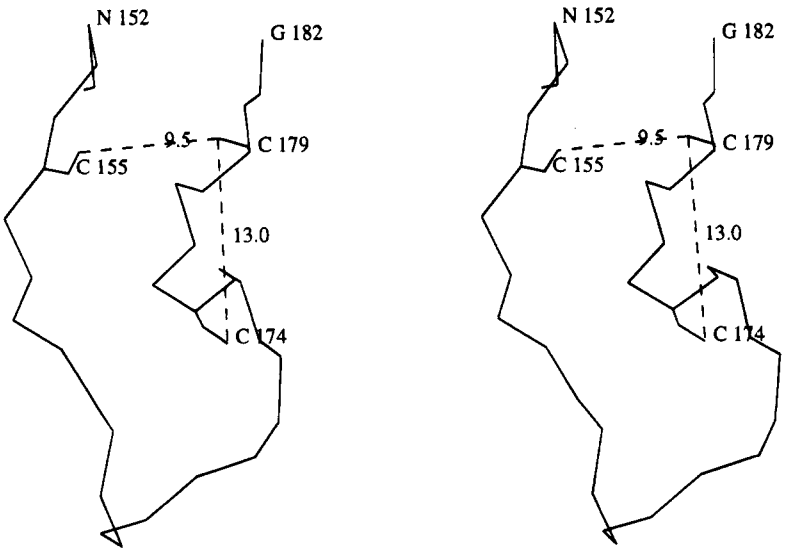

FIGURE 5: Stereoview showing the position of Cys^{155}, Cys^{174}, and Cys^{179} in monomer C2. Cα's of residues 152−182 are also shown. The Sγ atom of Cys^{179} is 9.5 and 13 Å apart from the Sγ atoms of Cys^{155} and Cys^{174}, respectively.

spinach chloroplast Fru-1,6-Pase shows a different position from that in the T and R states of the pig kidney enzyme, and this movement may have some implications for substrate binding and catalysis. However, further crystallographic studies of spinach chloroplast enzyme complexed with various substrates are required in order to investigate in detail the active sites of the enzyme.

DISCUSSION

The new quaternary conformation observed for spinach chloroplast Fru-1,6-Pase is outside of the pathway of the allosteric transition which occurs for the pig kidney enzyme and is closer to the T form than to the R form. Interestingly, a mutant form of hemoglobin, carbonmonoxyhemoglobin Ypsilanti, has been reported as having a quaternary structure which differs from any structures previously reported for hemoglobins and which can be described as more R than R: in this case the R state of normal hemoglobin lies between the T state of normal hemoglobin and the R state of carbonmonoxyhemoglobin Ypsilanti. It has been suggested (Smith et al., 1991) that this conformation may be visited in the T to R transition of normal hemoglobin, even though it is not in the direct pathway between T and R. This unusual structure for this mutant of hemoglobin may be similar to a low pH (less than 6) form of carbonmonoxyhemoglobin from the horse (M. Perutz, personal communication), and it remains questionable whether this third quaternary state occurs in the T to R transition of normal hemoglobin at physiological pH. A similar interpretation cannot be proposed for the spinach enzyme. Nevertheless, the new quaternary structure observed for this Fru-1,6-Pase suggests that the Fru-1,6-Pase tetramer has a great plasticity and may accommodate different conformations.

It has been generally assumed that chloroplast Fru-1,6-Pase is activated *in vivo* by reduction of disulfide groups via the thioredoxin reductase−thioredoxin *f* system (Buchanan, 1980). However, reduction of disulfide groups seems not to be the only process of regulation, and full activation of the enzyme can also be achieved without reducing agent, by Fru-2,6-P_2 and Mg^{2+} (Soulié et al., 1991). These activation processes are pH dependent, and the enzyme is fully active at pH 8.8 without any treatment (Zimmerman et al., 1976). Nevertheless, reduction of disulfide bridges seems to play an important role in the regulation of chloroplast Fru-1,6-Pase. Here we examine the location of cysteine residues in the three dimensional structure.

Seven cysteines are present within each monomer, in positions 51, 94, 155, 174, 179, 191, and 307 (Figure 1). On the basis of the present crystallographic structure, no disulfide bridge can be formed between cysteines belonging to two different monomers; the disulfide groups responsible for the regulation are present within one monomer itself. Within each monomer, two cysteines are clearly not involved in such an interaction: Cys^{94} and Cys^{307} have no cysteine residue in their close neighborhood. Three cysteines are located in the 170's loop (residues 158−174): cysteines in positions 155, 174, and 179. Cysteines 174 and 179 are separated only by four residues, a characteristic feature found in other enzymes containing redox-active cysteines, like mercuric reductase, glutathione reductase, lipoamide dehydrogenase, and $NADP^+$-malate dehydrogenase (Marcus et al., 1988). These cysteines are conserved among the five known sequences of chloroplast Fru-1,6-Pases from pea, spinach, wheat, *Arabidopsis thaliana*, and potato. Marcus et al. (1988) proposed that these cysteines may be involved in the light activation process. However, conservation of these residues among these five sequences is high (the sequence identity is between 80 and 90%), and all of the seven cysteines are preserved. The main differences occur only in the 170's loops which show different lengths. The 170's loops containing Cys^{155}, Cys^{174}, and Cys^{179} in the spinach chloroplast Fru-1,6-Pase have different extended conformations, and no disulfide bridge exists between residues 174 and 179: the two Sγ atoms are separated by 16, 13, 15, and 5 Å in monomers C1, C2, C3, and C4, respectively. Similarly, the Sγ atoms of Cys^{155} (at the beginning of the loop) are 7−18 Å away from Sγ atoms of Cys^{174} or Cys^{179} in the four monomers (Figure 5). A disulfide bridge cannot be formed between pairs of these cysteines without important conformational changes in the loops. In our crystallographic structure, these loops are involved in crystal packing interactions which can modify their three-dimensional conformations. However, the present

study suggests that some other disulfide groups may be involved in the slow conformational changes observed upon enzyme activation. We now briefly consider these disulfide groups.

Cysteines in position 51 and 191 are close to each other in the three-dimensional structure: the Sγ atoms of these two cysteines are separated only by 4.6 (C1), 3.9 (C2), 4.5 (C3), and 4.6 Å (C4). In the four monomers a simple rotation of the Sγ atom around the χ^1 torsion angle of cysteine 51 is sufficient to lower the distance between the two Sγ atoms to 2.4−2.7 Å. Cysteines 51 and 191 are found in helix H2 and strand B5, respectively (Figure 1). These two cysteine residues are located in the region which in the pig kidney enzyme forms the AMP binding site responsible for the allosteric behavior of this enzyme (helices H1, H2, H3, and the eight-stranded β-sheet). These two cysteines could form a disulfide bridge under adequate conditions. In our study, however, no density corresponding to a disulfide bridge was observed. It is not straightforward at the present time to compare our results from the X-ray diffraction with other biochemical studies. Site-directed mutagenesis of cysteines 51 and 191 and also cysteines 155, 174, and 179 should help to elucidate the exact role of these residues.

ACKNOWLEDGMENT

We thank Dr. H. Ke for his help in data collection and Dr. M. Nolte for critical reading of the manuscript.

REFERENCES

Ballicora, M. A., & Wolosiuk, R. A. (1990) *Plant Sci. 70*, 35−41.
Benkovic, S. J., & deMaine, M. M. (1982) *Adv. Enzymol. Relat. Areas Mol. Biol. 53*, 45−82.
Buchanan, B. B. (1980) *Annu. Rev. Plant, Physiol. 31*, 341−374.
Brunger, A. T. (1990) *Acta Crystallogr. A46*, 46−57.
Chardot, T., & Meunier, J.-C. (1991) *Biochem. J. 278*, 787−791.
Clancey, C. J., & Gilbert, H. F. (1987) *J. Biol. Chem. 262*, 13545−13549.
Francois, J., van Schaftingen, E., & Hers, H.-G. (1983) *J. Biol. Chem. 253*, 5712−5718.
Gomori, G. J. (1943) *J. Biol. Chem. 148*, 139−149.
Halliwell, B. (1981) in *Chloroplast Metabolism*, pp 66−68, Oxford University Press, New York.
Harbron, S., Foyer, C., & Walker, D. (1981) *Arch. Biochem. Biophys. 212*, 237−246.
Hertig, C., & Wolosiuk, R. A. (1980) *Biochem. Biophys. Res. Commun. 97*, 325−333.
Hertig, C. M., & Wolosiuk, R. A. (1983) *J. Biol. Chem. 258*, 984−989.
Herzog, B., Stitt, M., & Heldt, H. W. (1984) *Plant Physiol. 75*, 561−565.
Jones, T. A., Zou, J.-Y., Cowan, S. W., & Kjeldgaard, M. (1991) *Acta Crystallogr. A47*, 110−119.
Ke, H., Zhang, Y., & Lipscomb, W. N. (1990a) *Proc. Natl. Acad. Sci. U.S.A. 87*, 5243−5247.
Ke, H., Thorpe, C. M., Seaton, B. A., Lipscomb, W. N., & Marcus, F. (1990b) *J. Mol. Biol. 212*, 513−539.
Ke, H., Liang, J.-Y., Zhang, Y., & Lipscomb, W. N. (1991a) *Biochemistry 30*, 4412−4420.
Ke, H., Zhang, Y., Liang, J.-Y., & Lipscomb, W. N. (1991b) *Proc. Natl. Acad. Sci. U.S.A. 88*, 2989−2993.
Kirtley, M. E., & Dix, J. (1971) *Arch. Biochem. Biophys. 147*, 647−652.
Ladror, U. S., Latshaw, S. P., & Marcus, F. (1990) *Eur. J. Biochem. 189*, 89−94.
Liang, J.-Y., Huang, S., Zhang, Y., Ke, H., & Lipscomb, W. N. (1992) *Proc. Natl. Acad. Sci. U.S.A. 89*, 2404−2408.
Liang, J.-Y., Zhang, Y., Huang, S., & Lipscomb, W. N. (1993) *Proc. Natl. Acad. Sci. U.S.A. 90*, 2132−2136.
Marcus, F. (1981) in *The Regulation of Carbohydrate Formation and Utilization in Mammals* (Veneziale, C. M., Ed.) pp 269−290, University Park Press, Baltimore, MD.
Marcus, F., Harrsch, P. B., Moberly, L., Edelstein, I., & Latshaw, S. P. (1987) *Biochemistry 26*, 7029−7035.
Marcus, F., Moberly, L., & Latshaw, S. P. (1988) *Proc. Natl. Acad. Sci. U.S.A. 85*, 5379−5383.
Meunier, J.-C., Buc, J., Soulié, J.-M., Pradel, J., & Ricard, J. (1981) *Eur. J. Biochem. 113*, 513−520.
Navaza, J. (1993) *Acta Crystallogr. D49*, 588−591.
Pilkis, S. J., El-Maghrabi, M. R., Pilkis, J., & Claus, T. (1981) *J. Biol. Chem. 256*, 3619−3622.
Pradel, J., Soulié, J.-M., Buc, J., Meunier, J.-C., & Ricard, J. (1981) *Eur. J. Biochem. 113*, 513−520.
Preiss, J., Biggs, M. L., & Greenberg, E. (1967) *J. Biol. Chem. 242*, 2292−2294.
Smith, F. R., Lattman, E. E., & Carter, C. W., Jr. (1991) *Proteins 10*, 81−91.
Soulié, J.-M., Rivière, M., & Ricard, J. (1988) *Eur. J. Biochem. 176*, 111−117.
Soulié, J.-M., Rivière, M., Baldet, P., & Ricard, J. (1991) *Eur. J. Biochem. 195*, 671−678.
Tejwani, G. A. (1983) *Adv. Enzymol. Relat. Areas Mol. Biol. 54*, 121−194.
Van Schaftingen, E. (1987) *Adv. Enzymol. Relat. Areas Mol. Biol. 59*, 315−395.
Van Schaftingen, E., & Hers, H.-G. (1981) *Proc. Natl. Acad. Sci. U.S.A. 78*, 2861−2863.
Xue, Y., Huang, S., Liang, J.- Y., Zhang, Y., & Lipscomb, W. N. (1994) *Proc. Natl. Acad. Sci. U.S.A. 91*, 12482−12486.
Zhang, Y., Liang, J.-Y., Huang, S., Ke, H., & Lipscomb, W. N. (1993) *Biochemistry 32*, 1844−1857.
Zhang, Y., Liang, J.-Y., Huang, S., & Lipscomb, W. N. (1994) *J. Mol. Biol. 244*, 609−624.
Zhang, R., Chen, L. Villeret, V., & Fromm, H. (1995) *J. Biol. Chem. 270*, 54−58.
Zimmerman, G., Kelly, G. J., & Latzko, E. (1976) *J. Biol. Chem. 253*, 5952−5956.

BI942881Q